# Assessing T cell differentiation at the single-cell level

Gerlach, C.

7

# RECRUITMENT OF ANTIGEN-SPECIFIC CD8$^+$ T CELLS IN RESPONSE TO INFECTION IS MARKEDLY EFFICIENT

Jeroen W.J. van Heijst[1], Carmen Gerlach[1], Erwin Swart[1], Daoud Sie[2], Cláudio Nunes-Alves[3], Ron M. Kerkhoven[2], Ramon Arens[1], Margarida Correia-Neves[3], Koen Schepers[1] and Ton N.M. Schumacher[1]

[1]Division of Immunology and [2]Central Microarray Facility, the Netherlands Cancer Institute, Amsterdam, the Netherlands; [3]Life and Health Sciences Research Institute (ICVS), School of Health Sciences, University of Minho, Braga, Portugal

Science. 325:1265-9 (2009)

The magnitude of antigen-specific $CD8^+$ T cell responses is not fixed, but correlates with the severity of infection. Although by definition T cell response size is the product of both the capacity to recruit naïve T cells (clonal selection) and their subsequent proliferation (clonal expansion), it remains undefined how these two factors regulate antigen-specific T cell responses. Here we determined the relative contribution of recruitment and expansion by labeling naïve T cells with unique genetic tags and transferring them into mice. Under disparate infection conditions with different pathogens and doses, recruitment of antigen-specific T cells was near constant and close to complete. Thus, naïve T cell recruitment is highly efficient and the magnitude of antigen-specific $CD8^+$ T cell responses is primarily controlled by clonal expansion.

## INTRODUCTION, RESULTS & DISCUSSION

A key feature of adaptive immunity is its ability to recognize a wide range of pathogens by specific antigen receptors expressed on lymphocytes. Because the diversity of antigen receptors is large[1], the frequency of cells specific for any single antigen is extremely low (<1 in $10^5$ cells)[2,3]. This leaves the immune system with the remarkable challenge of selecting those few pathogen-specific cells amongst the millions of cells that do not recognize a given pathogen at the moment infection occurs. This process of 'clonal selection' is followed by massive expansion of those selected cells to give rise to sufficient progeny to combat the invading pathogen. Thus, the magnitude of adaptive immune responses is regulated by two processes. First, the number of participating clones is set by the efficiency with which antigen-specific cells are recruited from the naïve repertoire. Second, the burst size of these participating clones - defined as the net sum of all proliferation and cell death - determines the total number of antigen-specific progeny that is generated per recruited cell.



The magnitude of T cell responses generated upon infection is not fixed, but is shaped according to the severity of infection[4,5]. Although this correlation is well established, it remains undefined to what extent changes in the magnitude of response are the result of an effect on naïve T cell recruitment or clonal burst size. To quantify the number of recruited T cell clones in live infection models we have labeled individual naïve antigen-specific $CD8^+$ T cells with unique DNA sequences (barcodes)[6]. Because these barcodes are passed on to all daughter cells, this labeling strategy allowed us to distinguish the progeny of different recruited T cells within the total antigen-specific T cell pool that emerges during infection. Thus, the number of different barcodes detected within an antigen-specific T cell population directly correlates with the number of naïve T cells that have been recruited.

To first investigate the impact of pathogen dose on $CD8^+$ T cell recruitment, we labeled OT-I T cell receptor (TCR) transgenic T cells, which are specific for a peptide fragment of chicken ovalbumin presented by major histocompatibility class I, with a library of barcodes by retroviral transduction. We then transferred $10^3$ or $10^4$ barcode-labeled $GFP^+$ OT-I T cells into C57Bl/6 (B6) mice. One day later, we infected mice with different doses of recombinant *Listeria monocytogenes* bacteria expressing the chicken ovalbumin-derived $OVA_{257-264}$ epitope (LM-OVA) recognized by the OT-I TCR. At the peak of the $CD8^+$ T cell response (fig. S1), the total number of barcode-labeled $CD8^+$ T cells in spleens was determined. We observed a ten-fold increase in the magnitude of the $CD8^+$ T cell response between the lowest and the highest LM-OVA dose (Fig. 1A). In addition, a 10-fold increase in the number of antigen-specific precursors ($10^4$ OT-I T cells) at a fixed high pathogen dose resulted in a further (four-fold) increased T cell response.

To compare the efficiency of T cell recruitment under varying pathogen doses, we determined the number of different barcodes present within the OVA-specific $GFP^+$ T cell population. Barcodes were recovered by PCR and hybridized to

a barcode-microarray[6]. Analysis of microarray data showed that barcode content obtained from duplicate samples of a single mouse was highly reproducible, indicating that repertoire sampling was reliable (Fig. 1B). Furthermore, use of barcodes between different mice did not overlap. All barcode signals detected were derived from CD8$^+$ T cells that had been recruited into the immune response, as the signal from non-primed barcode-labeled cells was readily out-competed (fig. S2).



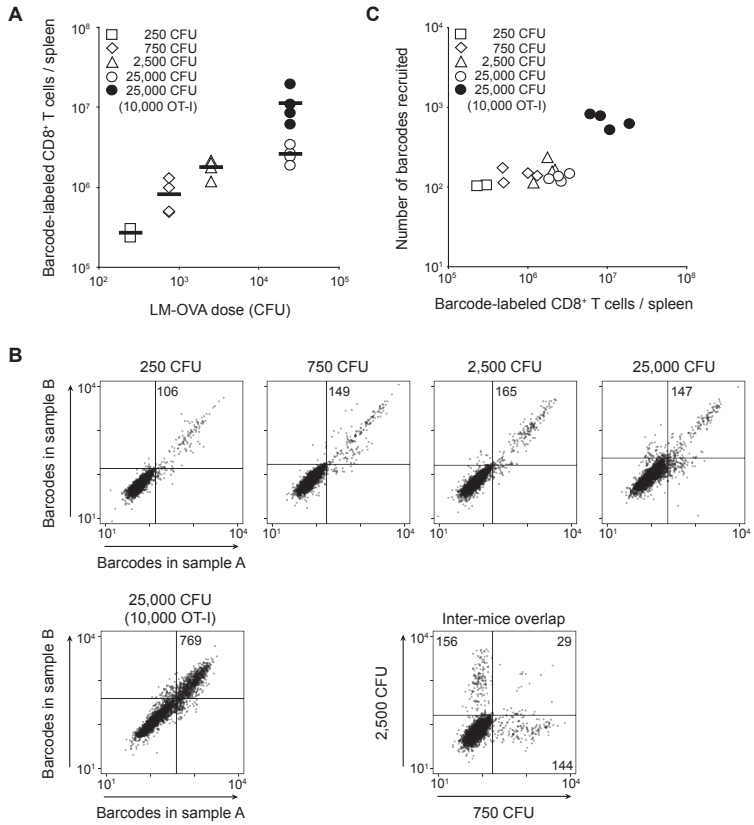


**Figure 1. Effect of pathogen dose and precursor frequency on CD8$^+$ T cell recruitment.** (**A**) Magnitude of the barcode-labeled CD8$^+$ T cell response. Recipients of $10^3$, or where indicated $10^4$, conA-activated GFP$^+$ barcode-labeled OT-I T cells were challenged with the indicated doses of LM-OVA. At the peak of the CD8$^+$ T cell response (day 8), the number of splenic barcode-labeled CD8$^+$ T cells was determined. Diamonds represent individual mice, bars represent group mean. (**B**) Barcode analysis of samples described in (A), showing representative barcode dot plots. In these plots each dot represents the fluorescent intensity of one barcode of the library. Values indicate the number of barcodes detected above background. Inter-mice comparison demonstrates that each mouse contains a unique set of barcodes. (**C**) Comparison of the magnitude of the CD8$^+$ T cell response to the number of antigen-specific precursors recruited for all individual mice. Data are representative of three independent experiments.

Interestingly, the number of different barcodes recovered from individual mice across the entire range of pathogen doses was highly comparable, with only a 1.5-fold difference in barcode numbers between the lowest and the highest LM-OVA dose (Fig. 1B). This indicates that the profoundly increased magnitude of the $CD8^+$ T cell response at higher pathogen dose occurs without a substantial increase in T cell recruitment. As the magnitude of a T cell response is the product of the number of T cell clones recruited and the burst size of each recruited clone, these data furthermore imply that clonal burst size was changed by seven-fold and thus forms the prime factor regulating T cell responses at varying pathogen dose (Fig. 1C). In contrast, when the available antigen-specific T cell repertoire was raised due to infusion of a larger number of T cell precursors, the observed increase in T cell response size (four-fold) was paralleled by an essentially proportional (five-fold) increase in the number of recruited barcodes (Fig. 1, B and C). Notably, near-constant recruitment of T cells at varying pathogen dose was also observed when naïve barcode-labeled OT-I T cells were generated in vivo, through injection of barcode-labeled OT-I thymocytes into the thymus of B6 recipients (fig. S3).



To determine whether near-constant recruitment also applies to other factors known to influence the magnitude of T cell responses, we addressed to what extent recruitment is affected by the duration of infection, or by pathogen type and route of infection. CFSE-dilution of OT-I T cells responding to LM-OVA infection revealed that Ampicillin antibiotic (Amp) treatment limits T cell priming to the first 72 hours post infection (fig. S4)[7]. To study how recruitment is affected by such a reduced duration of infection, recipients of naïve barcode-labeled OT-I T cells were challenged with LM-OVA with or without Amp treatment. Shortening the duration of infection reduced $CD8^+$ T cell responses by >ten-fold (Fig. 2A). However, the number of precursors recruited was only slightly lowered (~1.5-fold) (Fig. 2, B and C), indicating a change in clonal burst size by >seven-fold. Adoptive transfer of CFSE-labeled OT-I T cells from Amp-treated mice into either LM-OVA or wild-type LM-infected mice revealed that the enhanced clonal burst size observed upon prolonged infection is primarily due to increased T cell proliferation driven by sustained antigen exposure (fig. S5).

To examine whether near-constant recruitment occurs regardless of pathogen type or route of infection, recipients of naïve barcode-labeled OT-I T cells were challenged by either 1) systemic intravenous LM-OVA infection, 2) systemic intraperitoneal vaccinia virus-OVA infection, or 3) local intranasal influenza virus-OVA infection. A strong difference in the magnitude of $CD8^+$ T cell responses was observed, with the response to LM-OVA being >15-fold higher than the response to either vaccinia-OVA or influenza-OVA (Fig. 2D). Despite this major difference in T cell response, the number of recruited naïve T cells in response to these different pathogens was highly comparable (Fig. 2, E and F).

The above data indicate that T cell recruitment is highly constant, but do not reveal its efficiency. To directly enumerate recruitment efficiency, we quantified the number of antigen-specific T cells that do not undergo clonal expansion following infection. To

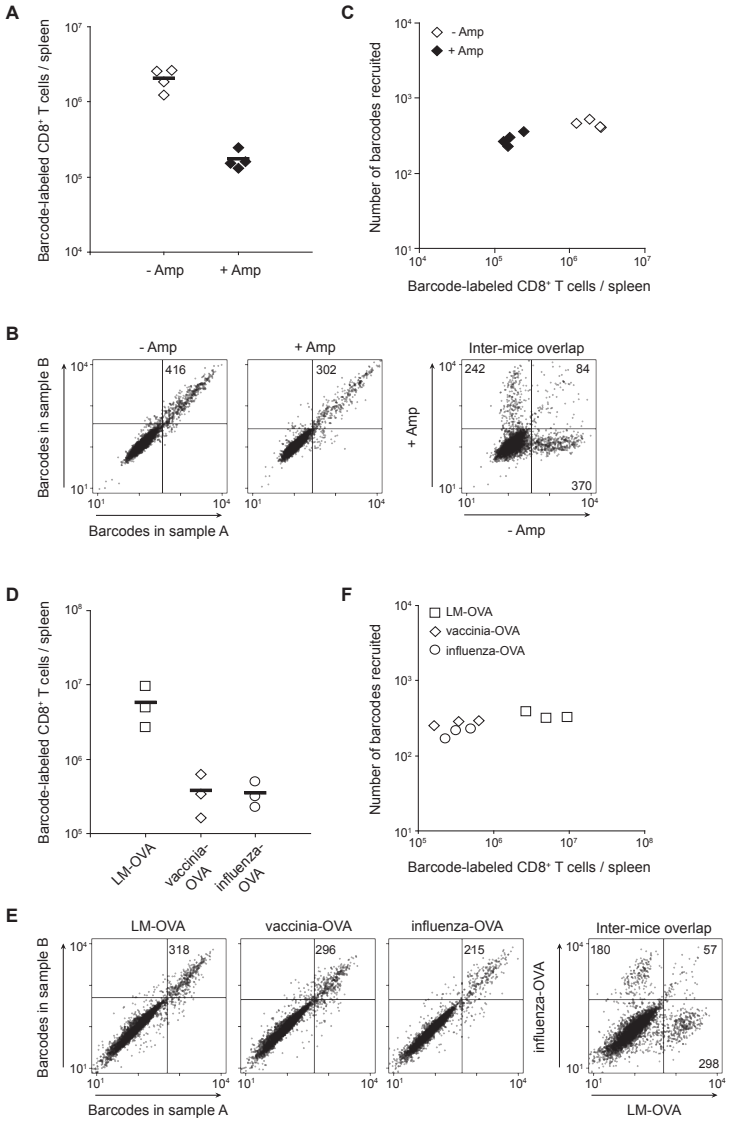


**Figure 2. Effect of duration of infection and pathogen type on CD8⁺ T cell recruitment.** (**A**) Magnitude of the barcode-labeled CD8⁺ T cell response of recipients of ~$10^3$ naïve barcode-labeled OT-I T cells that were infected with LM-OVA with or without Amp treatment. (**B**) Representative barcode dot plots of samples described in (A). (**C**) Comparison of the magnitude of the CD8⁺ T cell response to the number of antigen-specific precursors recruited for all individual mice. (**D**) Magnitude of the barcode-labeled CD8⁺ T cell response of recipients of ~$10^3$ naïve barcode-labeled OT-I T cells that were infected with LM-OVA, vaccinia-OVA, or influenza-OVA. (**E**) Representative barcode dot plots of samples described in (D). (**F**) Comparison of the magnitude of the CD8⁺ T cell response to the number of antigen-specific precursors recruited for all individual mice. Data are representative of two independent experiments.

this purpose, CD45.2 recipient mice received 5x10$^3$ CFSE-labeled congenic CD45.1$^+$ OT-I T cells and were challenged with either LM-OVA, wild-type LM, or left uninfected. Within the approximately 2x10$^7$ CD8$^+$ T cells recovered from pooled secondary lymphoid organs of wild-type LM-infected or uninfected mice at day 8 post infection, we detected on average 228 ± 24 and 288 ± 29 CFSE$^{hi}$ (non-recruited) OT-I T cells, respectively (Fig. 3). Importantly, in mice infected with LM-OVA only a very low number (8 ± 7) of remaining CFSE$^{hi}$ cells could be detected. This indicates that >95% of the OT-I T cell pool was selected to undergo clonal expansion when the OVA antigen was present and thus recruitment was close to complete.

Although the dissociation constant of the OT-I - K$^b$-OVA interaction ($K_d$ = 6μ M)[8] is representative of the interactions observed for T cells that recognize foreign antigens (0.1-20 μM)[9,10], it was important to establish whether polyclonal T cell populations expressing a range of TCR affinities follow similar patterns of recruitment. To address this issue, we made use of "Limited" (Ltd) mice that express the OT-I TCRα chain transgene together with a Vα2 TCRα chain minilocus[11]. Rearrangement of this minilocus has been shown to result in the formation of a restricted repertoire of CDR3α variants (~40 different TCRs were described in lymph node CD8$^+$ T cells). Consistent with the hypothesis that CD8$^+$ T cells of Ltd mice display variable affinities for the OVA antigen, Ltd CD8$^+$ T cells showed a range of K$^b$-OVA tetramer binding (Fig. 4A). Furthermore, similar to what was observed for OT-I cells (Fig. 1, fig. S3) and endogenous $OVA_{257-264}$-specific CD8$^+$ T cells (fig. S6), an increased magnitude of the Ltd CD8$^+$ T cell response was observed at increasing LM-OVA doses, with



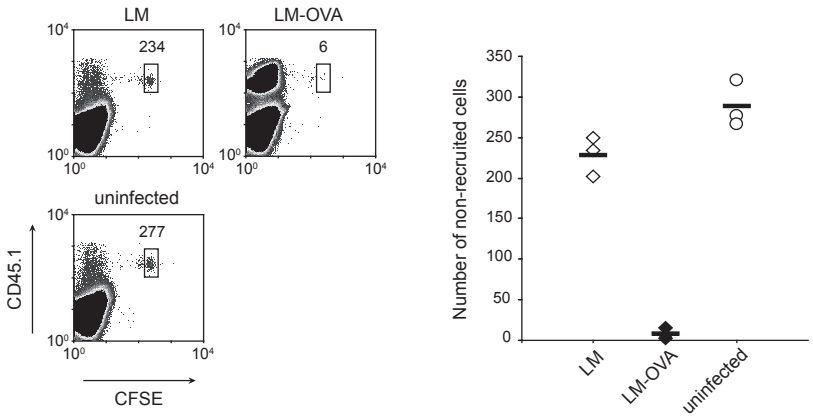


**Figure 3. Antigen-specific CD8$^+$ T cell recruitment upon infection is close to complete.** CD45.2 recipients of 5x10$^3$ CFSE-labeled CD45.1$^+$ OT-I T cells were infected with wild-type LM, LM-OVA, or left uninfected. At the peak of the CD8$^+$ T cell response, total spleen and lymph node CD8$^+$ T cells were analyzed by flow cytometry. Left: representative flow cytometry plots gated on live CD8$^+$ T cells; values indicate the number of non-recruited (CFSE$^{hi}$) OT-I T cells. Right: cumulative data for each group. Data are representative of six independent experiments.

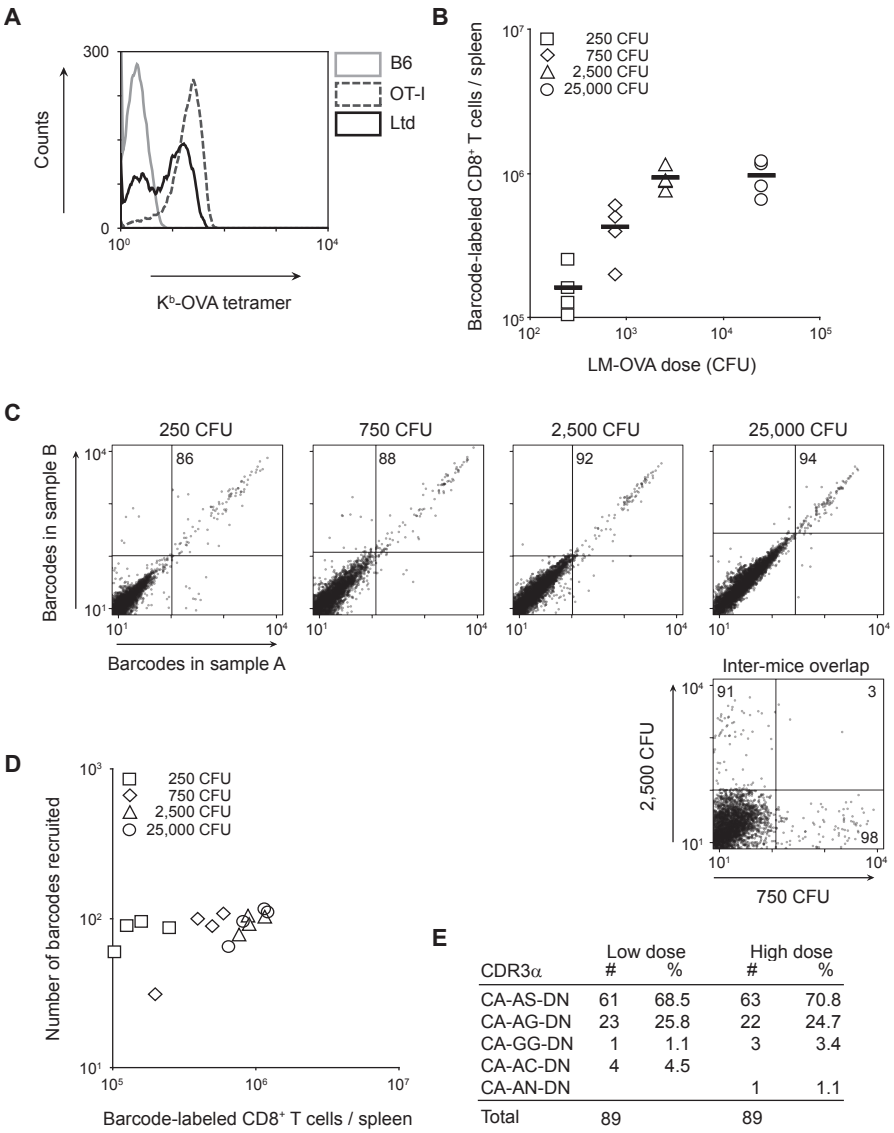


E

| CDR3α | Low dose # | Low dose % | High dose # | High dose % |
|---|---|---|---|---|
| CA-AS-DN | 61 | 68.5 | 63 | 70.8 |
| CA-AG-DN | 23 | 25.8 | 22 | 24.7 |
| CA-GG-DN | 1 | 1.1 | 3 | 3.4 |
| CA-AC-DN | 4 | 4.5 | | |
| CA-AN-DN | | | 1 | 1.1 |
| Total | 89 | | 89 | |

**Figure 4. Efficiency of T cell recruitment of polyclonal T cell populations.** (**A**) $K^b$-OVA tetramer binding of B6, OT-I and Ltd CD8+ T cells. Representative histogram gated on live CD8+ T cells is shown (two mice/group). (**B**) Magnitude of the barcode-labeled CD8+ T cell response of recipients of $10^3$ barcode-labeled Ltd CD8+ T cells that were challenged with indicated LM-OVA doses. (**C**) Representative barcode dot plots of samples described in (B). (**D**) Comparison of the magnitude of the CD8+ T cell response to the number of antigen-specific precursors recruited for all individual mice. (**E**) CDR3α TCR sequences of Ltd CD8+ T cells responding to infection. Data represent pooled sequences of two low (250 CFU) and two high dose (25,000 CFU)-infected mice. Note that the dominance of the CDR3α amino acid sequences CA-AS-DN and CA-AG-DN TCR (which comprise 35% and 19% of the naïve Ltd repertoire, respectively)[11], increases to a combined 95% upon antigen-driven selection.

a six-fold difference between the lowest and the highest dose (Fig. 4B). Nevertheless, recruitment of Ltd $CD8^+$ T cells was only minimally altered (<1.5 fold; Fig. 4, C and D). Importantly, both at low and high antigen dose, the vast majority of recruited Ltd cells was characterized by two TCRα protein sequences (94.3% and 95.5% of sequences, respectively) (Fig. 4E). Furthermore, the relative proportion of these two TCRα protein sequences in the responding T cell population was identical between low and high dose-challenged mice. Notably, these two TCRs, which have near-identical affinity for the OVA antigen (fig. S7), were both encoded by a high number of different CDR3α DNA sequences (table S1), indicating that these Ltd responses are highly polyclonal at the DNA level and selected for "fitness" at the protein level.

Under highly disparate conditions of infection, naïve $CD8^+$ T cell recruitment is near constant and close to complete. This indicates that control of the magnitude of antigen-specific $CD8^+$ T cell responses primarily occurs through regulation of clonal burst size. The observed efficiency of recruitment also indicates that the process through which naïve T cells scan antigen-presenting dendritic cells (DCs) must be sufficiently robust to allow the vast majority of antigen-specific T cells to encounter a DC carrying cognate antigen within the first 72 hours of infection. Assuming that naïve antigen-specific $CD8^+$ T cells are present at a frequency of ~1:100,000 within a $CD8^+$ T cell pool of ~$20x10^6$ cells, it would require around $59x10^6$ T-DC interactions to achieve 95% recruitment, a number that is largely independent of variations in precursor frequency within the physiological range (see Materials and methods). It has been estimated that DCs are able to interact with at least 500 different T cells/hour[12,13], thus a pool of <2,000 antigen-presenting DCs could suffice to achieve this near-complete recruitment.

How can participation of high affinity clones be highly efficient even at low pathogen dose, with little evidence for participation of additional clones at greatly increased pathogen levels? Previous studies of the $CD4^+$ T cell response to injected soluble antigens have shown that a high proportion of the TCR diversity found in the naïve repertoire was also preserved during the early stages of antigen-induced proliferation[2,14]. Notably, one of these studies showed that whereas early during the response TCR diversity was still highly reflective of the naïve repertoire, at the peak of the immune response TCR diversity was skewed towards higher affinity clones[14]. In line with this, recent data have shown that lower affinity interactions do result in T cell activation in vivo, but these responses undergo premature contraction[15]. Together with our data, these studies support a model in which the immune system maximizes its potential to react towards invading pathogens by allowing a near-complete recruitment of high affinity T cells, independent of the conditions of infection (fig. S8). Although this may lead to concomitant activation of lower affinity cells, the abortive expansion of these clones forms a filter against their further participation[14,15].

## MATERIALS AND METHODS

**Mice.** C57BL/6 (B6), OT-I T cell receptor (TCR) transgenic[16] and OT-I CD45.1 mice were bred in the animal facility of the Netherlands Cancer Institute. "Limited" (Ltd) mice[11] were bred in the animal facility of the ICVS, Portugal. Mice were maintained under specific pathogen-free conditions. All experiments were performed according to institutional and national guidelines, and were approved by the Experimental Animal Committee of the Netherlands Cancer Institute.

**Barcode library and microarray generation.** Generation of the barcode library and microarray has been described previously[6]. Briefly, the semi-random DNA stretch $(N_8\text{-}(SW)_5)_5\text{-}N_8$ was inserted 3' of the GFP sequence in the pLentilox3.4 vector. Following transformation, 4,743 *E. coli* cell clones were picked and individually expanded. The *E. coli* cell clones were pooled and subcloned into the pMX retroviral vector, to generate a Moloney-based retroviral barcode library. Next to this, barcodes from the individual *E. coli* cell clones were amplified by PCR and spotted in duplicate onto poly-L-lysine-coated glass slides to generate a barcode-microarray.



**Retroviral transduction.** Retroviral supernatants were generated using Phoenix-E packaging cells as described[17], and stored at -80°C. To generate barcode-labeled cells by *in vitro* retroviral transduction, OT-I or Ltd splenocytes were activated in IMDM (Invitrogen) supplemented with 8% heat-inactivated fetal calf serum, 100 U/ml penicillin plus 100 µg/ml streptomycin (Roche) and $0.5x10^{-5}$ M β-Mercaptoethanol (culture medium) in the presence of 2 µg/ml Concanavalin A (conA, Calbiochem) and 1 ng/ml IL-7 (Preprotech). After two days of culture, activated splenocytes were transduced with diluted retroviral supernatant by spin infection as described[17]. Retroviral supernatants were used at dilutions resulting in transduction efficiencies of 1-2%, at which the mean number of barcodes/cell is ~1.1 [6]. After O/N culture, cells were purified using Ficoll Paque Plus (Amersham Biosciences), stained with anti-CD8α-APC (BD, clone 53.6-7), and $GFP^+CD8\alpha^+$ cells were sorted on a FACSAria (BD) or MoFlo (Beckman Coulter). Sorted cells were washed in HBSS (Invitrogen) and injected intravenously ($10^3$ barcode-labeled T cells/mouse, unless indicated otherwise).

To generate naïve barcode-labeled OT-I T cells, OT-I thymocytes were transduced by spin infection in the presence of DOTAP transfection reagent (Roche) and 10 ng/ml IL-7 [18]. Four hours after transduction, cells were washed and incubated in DOTAP-free culture medium O/N. The next day, thymocytes were purified using Lympholyte-M (Cedarlane), and $GFP^+$ cells were sorted on a FACSAria or MoFlo. Sorted cells were washed in HBSS and injected intrathymically into anesthetized primary recipients (~$5x10^5$ barcode-labeled OT-I thymocytes/mouse). Three weeks later, spleen and lymph nodes of primary recipients containing mature naïve barcode-labeled OT-I T cells were pooled and enriched for $CD8^+$ T cells (BD IMag CD8 enrichment kit). Cells were washed in HBSS and injected intravenously into secondary recipients (~$10^3$ naïve barcode-labeled OT-I T cells/mouse).

Note that while we always aim to transfer $10^3$ thymocyte-derived naïve barcode-labeled OT-I T cells, this number is based on the analysis of the very low frequency of $GFP^+$ T cells within the primary recipients (~0.01% of $CD8^+$ cells), and therefore the actual number of transferred cells may show some variation. To ensure that all mice within a single experiment receive the same number of barcode-labeled cells, each mouse is reconstituted with an equal volume of donor cells from a single pool.

**Bacterial and viral infections.** Wild-type *Listeria monocytogenes* (LM) and *Listeria monocytogenes* that expresses a secreted form of OVA (LM-OVA)[19] were grown in brain heart infusion broth (BD) to an $OD_{600}$ of 0.1. For infections, mice were injected intravenously with $10^3$ colony-forming units (CFU) LM or $2.5x10^3$ CFU LM-OVA in HBSS, unless specified otherwise. *Listeria* doses were confirmed by plating dilutions on brain heart infusion agar (BD). Ampicillin (Amp) sodium salt treatment (Sigma) consisted of 1 mg Amp injected intraperitoneally at the start of infection, plus 2 mg/ml in the drinking water for 3-5 consecutive days. The recombinant vaccinia virus strain that expresses the full length OVA protein (vaccinia-OVA) has been described[20]. For infections, mice were injected intraperitoneally with $10^6$ plaque forming units (PFU) in HBSS. The recombinant influenza virus A/WSN/33 strain that expresses the H-$2K^b$-restricted $OVA_{257-264}$ epitope (influenza-OVA) has been described[21]. For infections, ether-anesthetized mice received an intranasal administration of $10^3$ PFU in HBSS.

**Quantification and purification of barcode-labeled T cells.** Spleens were isolated and homogenized by mincing through cell strainers (BD Falcon). The total number of barcode-labeled T cells was determined by counting spleen samples, staining with anti-Vα2-PE (BD, clone B20.1), and analysis of the percentage of $GFP^+V\alpha2^+$ T cells by flow cytometry. Live cells were selected based on propidium iodide exclusion. To purify barcode-labeled T cells from spleen samples, cells were stained with anti-Vα2-PE, labeled with anti-PE Microbeads (Miltenyi Biotec) and separated by MACS enrichment (Miltenyi Biotec).

**Barcode recovery, microarray hybridizations and data analysis.** Genomic DNA was isolated using a DNeasy tissue kit (Qiagen). To determine barcode sampling efficiency, barcode-containing gDNA samples were split into two equal parts (A and B) that were independently amplified by nested PCR[6]. PCR products were purified by MinElute columns (Qiagen), labeled with Cyanine-3 (Cy3) or Cyanine-5 (Cy5) fluorescent dyes (Kreatech) and hybridized to the barcode-microarray. Fluorescence intensities, as quantified using ImaGene 6.0 software (BioDiscovery, Inc.), were normalized, corrected for background noise, and duplicates were averaged. Barcode dot plots depict fluorescence intensities of the hybridized A and B samples, in which each dot represents one of the 4,743 barcodes present on the barcode-microarray. To quantify T cell recruitment, the number of barcodes with a signal above background with $P<0.05$ was determined by a one-sided *t*-test. The cut-offs used for this quantification are indicated by the dividers in the dot plots.

**CFSE-labeling.** Cell suspensions were washed in PBS/0.1% BSA and resuspended at $5x10^6$ cells/ml. CFSE (Molecular Probes) was added to a final concentration of 0.5-5 μM, and cells were incubated for 10 min at 37°C. Following quenching by addition of ice-cold culture medium, cells were washed in fresh medium, resuspended in HBSS, and injected intravenously into mice. For analysis, the indicated lymphoid organs were homogenized and erythrocytes were removed by ammonium chloride treatment. Cells were stained with anti-CD8α-PE-Cy7 (BD, clone 53.6-7) and anti-CD45.1-APC (Southern Biotech, clone A20), and analyzed by flow cytometry on a CyAnADP (Beckman Coulter). Analysis was performed using Summit V4.3 software (Beckman Coulter).

**TCR cloning and sequence analysis.** OT-Iα chain variants encoding the CDR3α amino acids sequences CA-AS-DN, CA-AG-DN and CA-ARE-DN were ordered at GeneArt (Regensburg, Germany) and cloned into the pMX retroviral vector in front of an IRES-OT-Iα chain cassette. Retroviral supernatants were used to transduce conA-activated B6 splenocytes with the indicated TCRs. Transduction efficiency was determined by staining with anti-Vβ5-FITC (BD, clone MR9-4) and anti-Vα2-PE antibodies. Intracellular IFN-γ staining to determine functionality was performed using a Cytofix/Cytoperm with GolgiPlug kit (BD). To analyze the TCR repertoire of recruited Ltd $CD8^+$ T cells, responding cells were sorted based on anti-Vβ5-FITC, anti-CD45.2-PE (eBioscience, clone 104) and anti-CD8α-APC staining. gDNA from sorted cells was isolated and CDR3α regions were amplified by nested PCR using the following primers (5' to 3'): top –CAGCAGCAGGTGAGACAAAGT– and bottom –ATCGGCTGAGTGCATTGTCT– in the first round; top –TCCATACGTTCAGTGTCCGATAAA– and bottom –GGCTTTATAATTAGCTTGGTCCCAGAG– in the second round, with a 50°C annealing temperature. PCR products were cloned using TOPO TA cloning (Invitrogen) and individual colonies were analyzed by BigDye Terminator sequencing (Applied Biosystems).

**Calculating T-DC interaction requirements for efficient recruitment.** The number of T-DC interactions required to recruit 95% of antigen-specific T cells was calculated as follows. If X = the total number of $CD8^+$ T cells and Y = the number of antigen-specific $CD8^+$ T cells, then X/Y defines the average number of interactions required to recruit a first antigen-specific T cell. As this cell is now depleted from both the total T cell pool as well as from the antigen-specific T cell pool, the second recruitment event requires on average X-1/Y-1 interactions. These calculations can be continued until 95% of Y has been recruited. The sum of the interaction events required for each subsequent recruitment event provides the total number of T-DC interactions required to recruit 95% of antigen-specific T cells present at a precursor frequency of Y/X. As exemplified in the main text, assuming $X = 20x10^6$ and Y = 200, then ~$59x10^6$ T-DC interactions are required to achieve 95% recruitment. Interestingly, this number is largely independent of variations in precursor frequency within the physiological range, as 95% recruitment at a frequency of 1:200,000 (100 antigen-specific cells/mouse) or 1:20,000 (1,000 antigen-specific cells/mouse) would require ~$58x10^6$ and ~$60x10^6$ T-DC interactions, respectively.

## ACKNOWLEDGMENTS

We thank F. van Diepen and A. Pfauth for cell sorting, D. Busch for LM-OVA, W. Brugman for microarray production and N. Armstrong for statistical help. We thank S. Naik and V. Ganusov for discussions and H. Jacobs, G. Bendle, J. Shu, M. Wolkers and S. Ariotti for reading the manuscript. GenBank accession numbers are FI903161 to FI903338.

## REFERENCE LIST

1. Casrouge, A. *et al*. Size estimate of the alpha beta TCR repertoire of naive mouse splenocytes. *J. Immunol.* 164, 5782-5787 (2000).
2. Moon, J. J. *et al*. Naive CD4(+) T cell frequency varies for different epitopes and predicts repertoire diversity and response magnitude. *Immunity* 27, 203-213 (2007).
3. Obar, J. J., Khanna, K. M. & Lefrancois, L. Endogenous naive CD8+ T cell precursor frequency regulates primary and memory responses to infection. *Immunity* 28, 859-869 (2008).
4. Badovinac, V. P., Porter, B. B. & Harty, J. T. Programmed contraction of CD8(+) T cells after infection. *Nat. Immunol.* 3, 619-626 (2002).
5. Prlic, M., Hernandez-Hoyos, G. & Bevan, M. J. Duration of the initial TCR stimulus controls the magnitude but not functionality of the CD8+ T cell response. *J. Exp. Med.* 203, 2135-2143 (2006).
6. Schepers, K. *et al*. Dissecting T cell lineage relationships by cellular barcoding. *J. Exp. Med.* 205, 2309-2318 (2008).
7. Mercado, R. *et al*. Early programming of T cell populations responding to bacterial infection. *J. Immunol.* 165, 6833-6839 (2000).
8. Alam, S. M. *et al*. Qualitative and quantitative differences in T cell receptor binding of agonist and antagonist ligands 50. *Immunity* 10, 227-237 (1999).
9. Davis, M. M. *et al*. Ligand recognition by alpha beta T cell receptors 51. *Annu. Rev. Immunol.* 16, 523-544 (1998).
10. Cole, D. K. *et al*. Human TCR-binding affinity is governed by MHC class restriction 67. *J. Immunol.* 178, 5727-5734 (2007).
11. Correia-Neves, M., Waltzinger, C., Mathis, D. & Benoist, C. The shaping of the T cell repertoire 59. *Immunity* 14, 21-32 (2001).
12. Bousso, P. & Robey, E. Dynamics of CD8+ T cell priming by dendritic cells in intact lymph nodes. *Nat. Immunol.* 4, 579-585 (2003).
13. Beltman, J. B., Maree, A. F., Lynch, J. N., Miller, M. J. & de Boer, R. J. Lymph node topology dictates T cell migration behavior. *J. Exp. Med.* 204, 771-780 (2007).
14. Malherbe, L., Hausl, C., Teyton, L. & McHeyzer-Williams, M. G. Clonal selection of helper T cells is determined by an affinity threshold with no further skewing of TCR binding properties. *Immunity* 21, 669-679 (2004).
15. Zehn, D., Lee, S. Y. & Bevan, M. J. Complete but curtailed T-cell response to very low-affinity antigen. *Nature* 458, 211-214 (2009).
16. Hogquist, K. A. *et al*. T cell receptor antagonist peptides induce positive selection. *Cell* 76, 17-27 (1994).
17. Kessels, H. W., Wolkers, M. C., van den Boom, M. D., van der Valk, M. A. & Schumacher, T. N. Immunotherapy through TCR gene transfer. *Nat. Immunol.* 2, 957-961 (2001).
18. Gerlach, C. *et al*. One naïve T cell, multiple fates in CD8$^+$ T cell differentiation. *J. Exp. Med.* 207, 1235-1246 (2010).
19. Pope, C. *et al*. Organ-specific regulation of the CD8 T cell response to Listeria monocytogenes infection. *J. Immunol.* 166, 3402-3409 (2001).
20. Restifo, N. P. *et al*. Antigen processing in vivo and the elicitation of primary CTL responses 66. *J. Immunol.* 154, 4414-4422 (1995).
21. Topham, D. J., Castrucci, M. R., Wingo, F. S., Belz, G. T. & Doherty, P. C. The role of antigen in the localization of naive, acutely activated, and memory CD8(+) T cells to the lung during influenza pneumonia. *J Immunol* 167, 6983-6990 (2001).

**Table S1. CDR3α DNA sequences of recruited Ltd CD8⁺ T cells.**

| CDR3α AS encoded by | | Low dose | | High dose | | CDR3α AG encoded by | | Low dose | | High dose | |
|---|---|---|---|---|---|---|---|---|---|---|---|
| | | # | % | # | % | | | # | % | # | % |
| GCA | AGT | 51 | 83.6 | 52 | 82.5 | GCA | GGT | 14 | 60.9 | 11 | 50.0 |
| GCC | TCT | 3 | 4.9 | 4 | 6.3 | GCG | GGG | 2 | 8.7 | 3 | 13.6 |
| GCA | AGC | 3 | 4.9 | 3 | 4.8 | GCG | GGT | 2 | 8.7 | 1 | 4.5 |
| GCA | TCC | 4 | 6.6 | | | GCA | GGG | 1 | 4.3 | 2 | 9.1 |
| GCA | TCT | | | 2 | 3.2 | GCA | GGC | 3 | 13.0 | | |
| GCT | TCT | | | 1 | 1.6 | GCA | GGA | 1 | 4.3 | | |
| GCG | TCC | | | 1 | 1.6 | GCT | GGT | | | 2 | 9.1 |
| | | | | | | GCT | GGG | | | 1 | 4.5 |
| | | | | | | GCC | GGT | | | 1 | 4.5 |
| | | | | | | GCC | GGG | | | 1 | 4.5 |
| **Total** | | **61** | | **63** | | | | **23** | | **22** | |

CDR3α DNA sequences of Ltd CD8⁺ T cells recruited into the response upon either low or high dose LM-OVA infection. Data represent pooled sequences from two low and two high dose-infected mice.

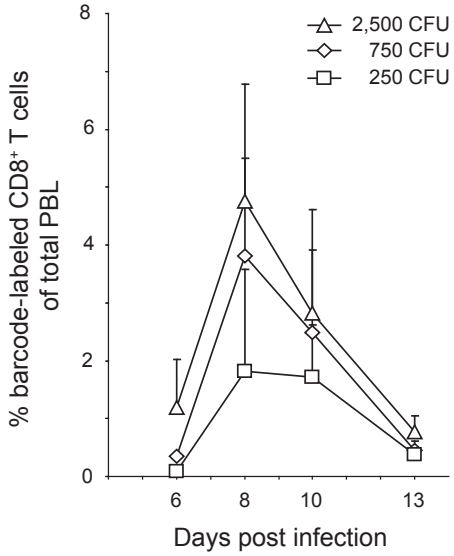


**Figure S1. Kinetics of peripheral blood CD8⁺ T cell responses upon challenge with different LM-OVA doses.** Mice received $10^3$ conA-activated barcode-labeled OT-I T cells and were infected with the specified doses of LM-OVA. On the indicated days post infection, the percentage of barcode-labeled CD8⁺ T cells in peripheral blood was determined. Symbols indicate group averages + s.d. of three mice/group.

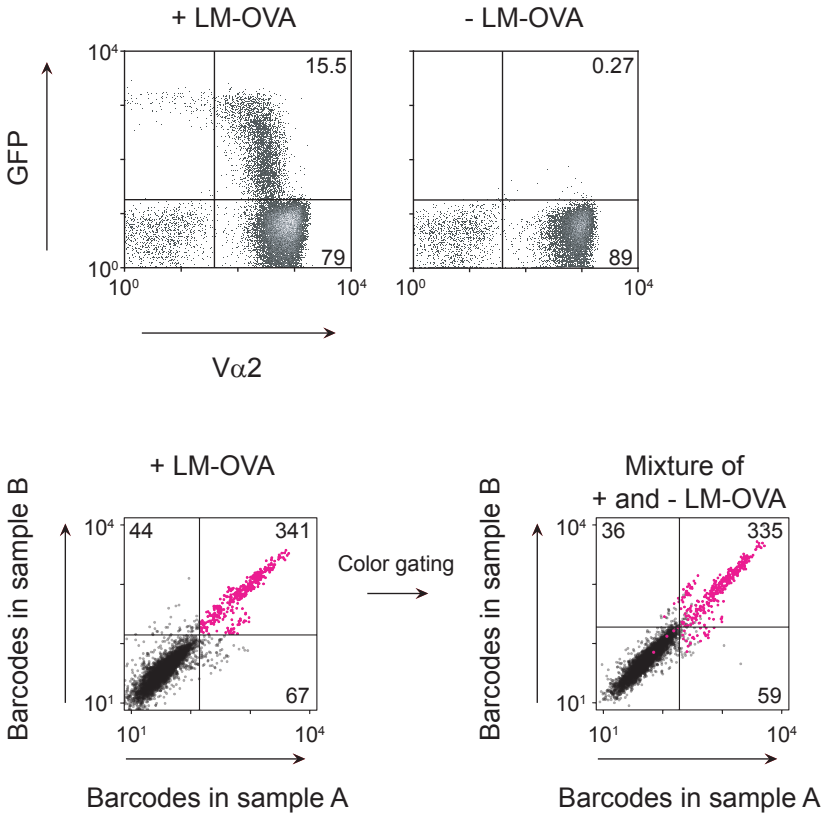


**Figure S2. Detection by barcode-microarray is restricted to barcodes of T cells that have been recruited into the immune response.** Mice received $10^3$ conA-activated barcode-labeled OT-I T cells and were either infected with LM-OVA (+ LM-OVA) or not infected (- LM-OVA). At the peak of the $CD8^+$ T cell response, splenic $V\alpha2^+$ T cells (i.e. barcode-labeled OT-I T cells plus endogenous $V\alpha2^+$ T cells) were enriched by magnetic separation and used for flow cytometry and barcode analysis. Top panel: flow cytometry plots indicating the percentage of barcode-labeled ($GFP^+$) cells vs. non-barcode-labeled cells after Vα2 enrichment. Bottom panel: gDNA was isolated and barcode PCR amplifications were performed on either the + LM-OVA gDNA sample, or on a 1:1 mixture of the + LM-OVA and – LM-OVA gDNA sample. Resulting PCR products were hybridized to the barcode-microarray. Barcodes present above background in the + LM-OVA dot plot were color-labeled and gated to the + and – LM-OVA dot plot to determine to what extent the barcodes from the + LM-OVA sample dominated the combined sample. Values indicate the number of barcodes detected above background. Note that essentially all barcodes recovered from the mixed sample are derived from the + LM-OVA sample.

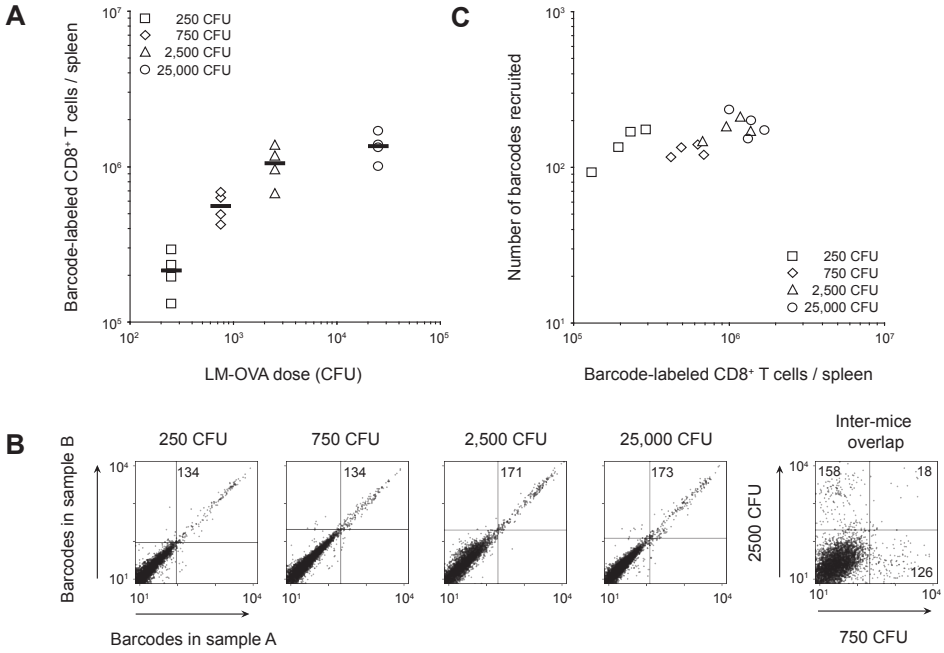


**Figure S3. Effect of pathogen dose on naïve CD8⁺ T cell recruitment.** (**A**) Magnitude of the barcode-labeled CD8⁺ T cell response of mice that received ~$10^3$ naïve barcode-labeled OT-I T cells and were challenged with the indicated doses of LM-OVA. (**B**) Barcode analysis of samples described under (A), showing representative barcode dot plots for each pathogen dose. Inter-mice comparison demonstrates that each mouse contains a unique set of barcodes. (**C**) Comparison of the magnitude of the CD8⁺ T cell response to the number of antigen-specific precursors recruited for all individual mice.

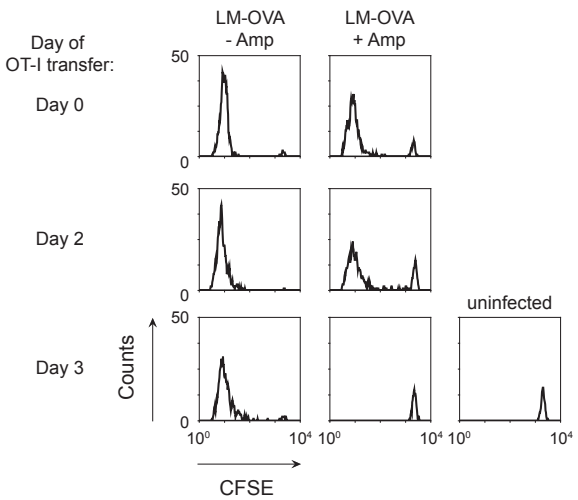


**Figure S4. Kinetics of $OVA_{257-264}$ antigen presentation after LM-OVA infection and antibiotic treatment.** $10^6$ CFSE-labeled CD45.1⁺ OT-I T cells were transferred into CD45.2 recipients at various time points post LM-OVA infection with or without Amp treatment. Four days after transfer, T cell proliferation was measured by analysis of CFSE dilution of recovered spleen cells. Representative histograms gated on donor CD8⁺ CD45.1⁺ OT-I T cells are depicted (two mice/group).

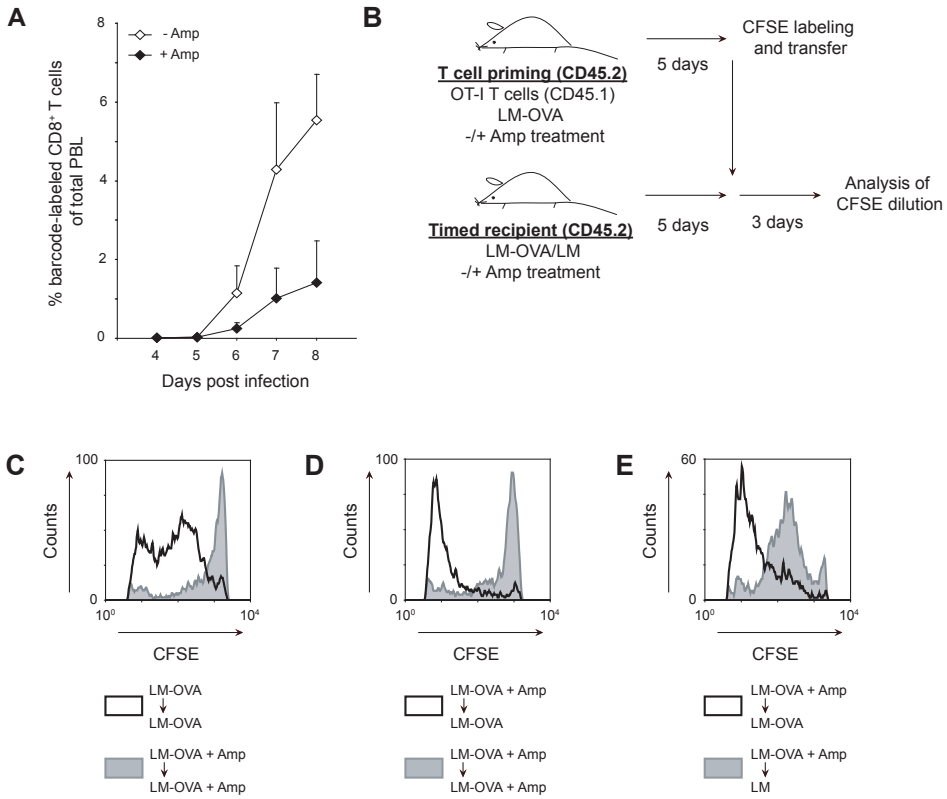


**Figure S5. Enhanced CD8⁺ T cell burst size is driven by sustained antigen exposure.** (**A**) Kinetics of peripheral blood CD8⁺ T cell responses after LM-OVA infection with or without antibiotic treatment. Mice received ~$10^3$ naïve barcode-labeled OT-I T cells, were infected with LM-OVA and were treated with or without Amp. Data depict the percentage of barcode-labeled CD8⁺ T cells in peripheral blood at the indicated time points. Diamonds indicate group averages + s.d. of four mice/group. (**B**) General set-up of the adoptive transfer experiments depicted in (C-E). CD45.2 mice received $10^3$ CD45.1⁺ OT-I T cells, were infected with LM-OVA, and were either left untreated (- Amp) or treated with Amp (+ Amp; T cell priming group). Concomitantly, CD45.2 mice were infected with the indicated LM strain with or without Amp treatment, however without receiving any OT-I T cells (timed recipient group). At day 5 post infection, spleen cells from T cell priming mice were isolated, labeled with CFSE, and transferred into timed recipient mice. Three days later, CD45.1⁺ OT-I T cells in spleens of timed recipient mice were analyzed for CFSE dilution. (**C**) Cells from LM-OVA 'primed' mice without Amp treatment and cells from LM-OVA 'primed' mice with Amp treatment were each transferred into matched timed recipient mice. (**D**) Cells from LM-OVA 'primed' mice with Amp treatment were transferred into either untreated or Amp-treated timed recipient mice. (**E**) Cells from LM-OVA 'primed' mice with Amp treatment were transferred into either LM-OVA or LM-infected timed recipient mice. (**C**-**E**) Representative histograms gated on donor CD8⁺ CD45.1⁺ OT-I T cells are shown (two mice/group). Note that primed T cells transferred into LM-infected mice proliferate more than cells transferred into LM-OVA Amp-treated mice (compare gray histograms of C and D to E), indicating that inflammation in the absence of cognate antigen also does sustain T cell proliferation to some extent.

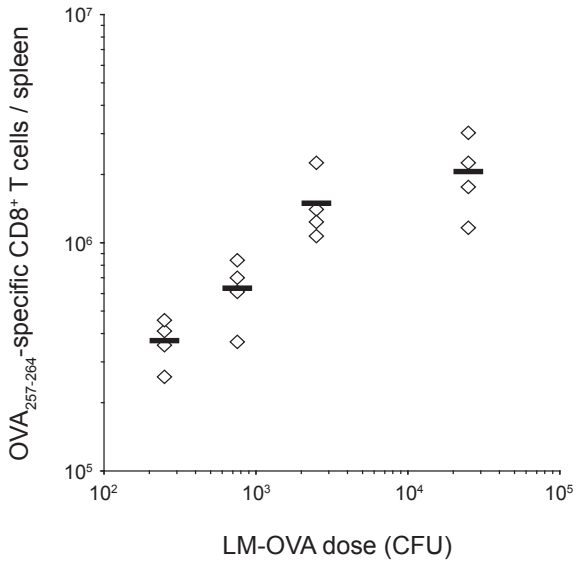


**Figure S6. Effect of pathogen dose on endogenous OVA-specific CD8⁺ T cell responses.** Mice were challenged with the indicated doses of LM-OVA. At the peak of the CD8⁺ T cell response, the magnitude of the splenic $OVA_{257-264}$-specific CD8⁺ T cell response was determined by $K^b$-OVA tetramer staining. Diamonds represent individual mice, bars represent group averages.

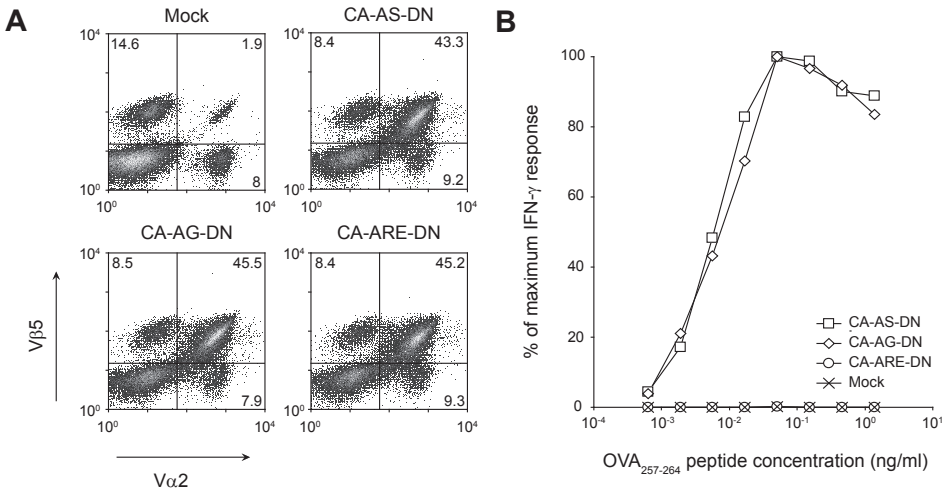


**Figure S7. Antigen sensitivity of T cells expressing Ltd CDR3α variants.** (**A**) B6 splenocytes were transduced with TCR constructs expressing the indicated Ltd CDR3α variants. FACS plots depicting the transduction efficiency of gated live CD8⁺ T cells are shown. (**B**) Intracellular IFN-γ staining of indicated TCR-transduced cell populations after stimulation with $OVA_{257-264}$ peptide. Data represents the dose-response curve normalized to the maximum percentage of IFN-γ producing cells for each cell population. Note that for the CA-ARE-DN TCR (the third most prevalent TCR in the Ltd naïve repertoire)[11] and mock-transduced cells no specific IFN-γ production above background was detected.

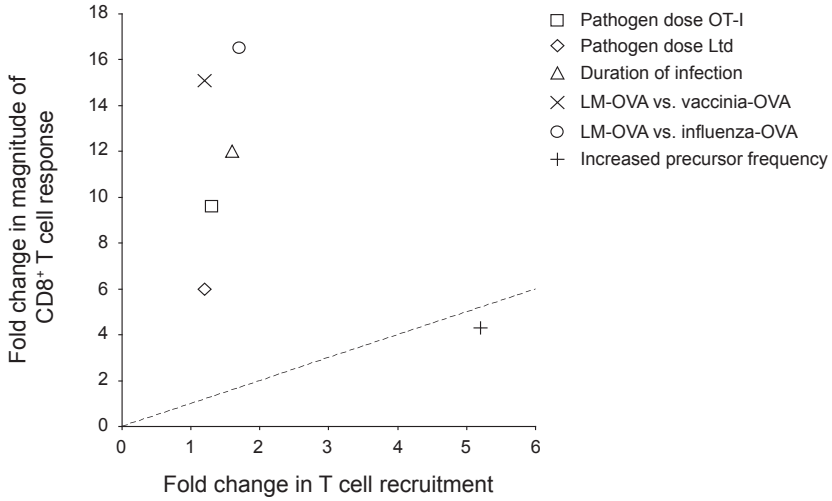




**Figure S8. Variations in pathogen dose, duration of infection and pathogen type strongly affect the magnitude of the CD8⁺ T cell response, while naïve T cell recruitment remains near constant.** Data from Fig. 1 (lowest versus highest pathogen dose), Fig. 2 and Fig. 4 (lowest versus highest pathogen dose) were converted to plot the average fold change in T cell recruitment against the average fold change in the magnitude of the T cell response. The trend line indicates the predicted correlation in case variation in T cell response size would be fully explained by changes in T cell recruitment. Note that of all parameters tested, the magnitude of the T cell response only correlates with T cell recruitment in case T cell precursor frequency is altered.